SF2A 2018
P. Di Matteo, F. Billebaud, F. Herpin, N. Lagarde, J.-B. Marquette, A. Robin, O. Venot (eds)

CHARACTERIZING THE PHOTOSPHERIC CONVECTION OF RED SUPERGIANT STARS AT HIGH ANGULAR RESOLUTION

M. Montargès[1], R. Norris[2], B. Tessore[3], A. López Ariste[4], A. Chiavassa[5] and A. Lèbre[6]

Abstract. Over the past few years, our knowledge of red supergiant stars has changed dramatically thanks to the development of high angular resolution techniques (interferometry in both the optical and mm domains, adaptive optics) and of numerical modeling. We present here our last results on the observation of the photosphere of red supergiants using near infrared interferometry and visible spectropolarimetry.

Keywords: stars: imaging, supergiants, stars: mass-loss, infrared: stars, techniques: interferometric

1 Introduction

Mass loss of evolved stars is the main contributor to the chemical enrichment of the Universe. It also has consequences on the ultimate fate of the star. For massive stars (> 8 $M_\odot$), the mass loss rate during the red supergiant (RSG) stage will determine the mass, hence the nature, of the remnant compact object but also the structure of the supernova remnant. Before this ultimate stage, Meynet et al. (2015) showed that the mass loss rate has critical consequences on the evolutionary path taken by the star in its final stages.

However, little is known about the mechanism triggering the mass loss of RSG stars. A 2.5-D magnetohydrodynamic (MHD) model was able to reproduce the terminal wind velocity of the prototypical RSG Betelgeuse using the dissipation of Alvén waves in the chromosphere (Airapetian et al. 2000). However, Josselin & Plez (2007) proposed that photospheric convection could lower the effective gravity and allow the radiative pressure on molecular lines to trigger the outflow. Both mechanisms received partial confirmations when the magnetic field of Betelgeuse was detected (Aurière et al. 2010), and then followed over several years (Mathias et al. 2018), thus indicating the feasibility of the first scenario. A possible convection related event was observed by a combination of observations of Betelgeuse with VLTI/PIONIER (Montargès et al. 2016), VLT/SPHERE (Kervella et al. 2016), and ALMA (O'Gorman et al. 2017; Kervella et al. 2018).

We present here observations of the photosphere of several RSG using near infrared (NIR) interferometry (Sect. 2). These results are compared with visible spectropolarimetric data in Sect. 3. Finally our concluding remarks are summarized in Sect. 4.

2 NIR interferometric observations of RSG

In this section, we briefly present RSG observations recently obtained with NIR interferometry. As we are interested in the photospheric structures, the two stars we will be discussing are both nearby RSG.

[1] Institute of Astronomy, KU Leuven, Celestijnenlaan 200D B2401, 3001 Leuven, Belgium
[2] Department of Physics and Astronomy, Georgia State University, PO Box 5060 Atlanta, GA 30302-5060, USA
[3] Univ. Grenoble Alpes, CNRS, IPAG, 38000 Grenoble, France
[4] IRAP, Université de Toulouse, CNRS, CNES, UPS., 14, Av. E. Belin., 31400 Toulouse, France
[5] Université Côte d'Azur, Observatoire de la Côte d'Azur, CNRS, Lagrange, CS 34229, Nice, France
[6] Université de Montpellier, CNRS, LUPM, Place E. Bataillon, 34090 Montpellier, France

2.1 Betelgeuse (α Ori) with VLTI/PIONIER

Betelgeuse is the prototypical M2 RSG in the Orion constellation. It is located at 222^{+48}_{-34} pc (Harper et al. 2017) and an effective temperature of 3690 ± 54 K (Ohnaka et al. 2011) It was observed with VLTI/PIONIER (Le Bouquin et al. 2011) on 01 February 2012, 10 February 2013, 12 January 2014 and 22 November 2014. The data were reduced using the public PIONIER pipeline. The interferometric observables showed significant departure from spherical symmetry (position angle dependent diameter, and closure phase values different from 0 and 180 degrees).

The best fitted models correspond to a combination of a limb darkened disk and a bright Gaussian spot (see Fig. 1 and Montargès et al. 2016). The evolution of the bright Gaussian spot is followed from February 2012 to January 2014 on the Eastern side of the star. After that it seems to have been replaced by another one on the Western side.

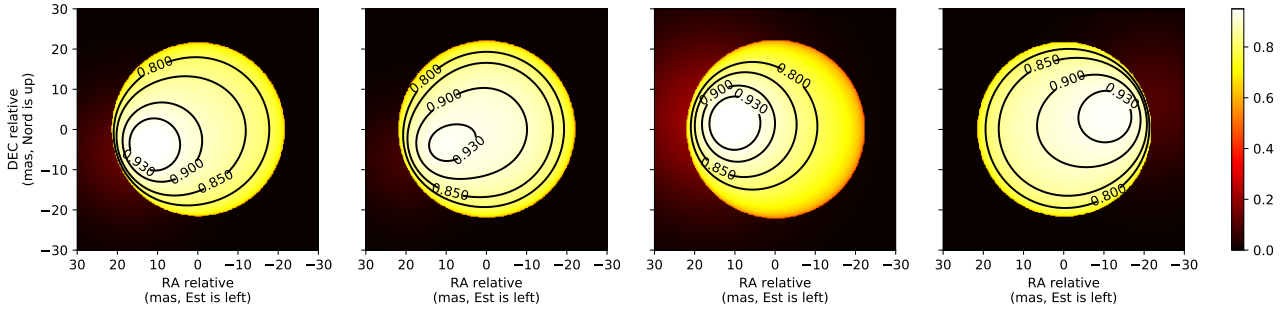

Fig. 1. Intensity maps of the best fitted model matching the VLTI/PIONIER observations of Betelgeuse for the different observed epochs in (from left to right, February 2012, February 2013, January 2014, and November 2014; see Montargès et al. 2016).

In the past, 3D radiative models were successfully reproducing interferometric observations by producing convective cells on the photosphere (Chiavassa et al. 2010; Montargès et al. 2014). However, for these PIONIER data, the same convective simulations (Chiavassa et al. 2011) are not able to produce such giant bright features.

2.2 CE Tau with VLTI/PIONIER

CE Tau is M2 RSG with a parallax of 1.82 ± 0.26 mas (van Leeuwen 2007) and an effective temperature of $3801 - 3820 \pm 135$ K (Montargès et al. 2018). We observed this star with VLTI/PIONIER in November and December 2016 (Montargès et al. 2018). The well sampled (u, v) plane allowed for image reconstruction that was performed using the `SQUEEZE` algorithm (Baron et al. 2010). The reconstructed images were tested against possible biases using synthetic observations of 3D RHD simulations, and by obtaining similar images with the `MIRA` reconstruction algorithm (Thiébaut 2008).

The `SQUEEZE` images are represented on Fig 2. Several features are visible, particularly a bright one near the disk center and a dark one to South East. The interferometric observables are compatible with 3D RHD simulations. However, the intensity contrast $\delta I_{\rm rms}/\langle I \rangle$ (defined in Tremblay et al. 2013) is lower in the reconstructed images compared to the simulations. We interpret this as a result of the lower effective temperature and surface gravity of the simulations which lead to a more prominent simulated convective pattern. Generating this 3D RHD full stellar simulations requires a lot of computational capabilities but we hope to get specifically tailored simulations in the future. It is also possible that CE Tau is currently experiencing a quiet convective episode. This can only be determined by further temporal monitoring.

3 Comparison with visible spectropolarimetry

Both stars were observed by TBL/Narval within some days preceding or following our interferometric observations. Using a mask of 15 000 atomic lines and a least-squares deconvolution approach (LSD, Donati et al. 1997), it was possible to clearly detect the linear polarization associated to the spectrum. By noticing that the Na I D1 line had a stronger polarization than the D2 line, while the D2 line has the highest polarizability, Aurière et al. (2016) interpreted the polarization in the lines as a depolarization of the continuum. As the

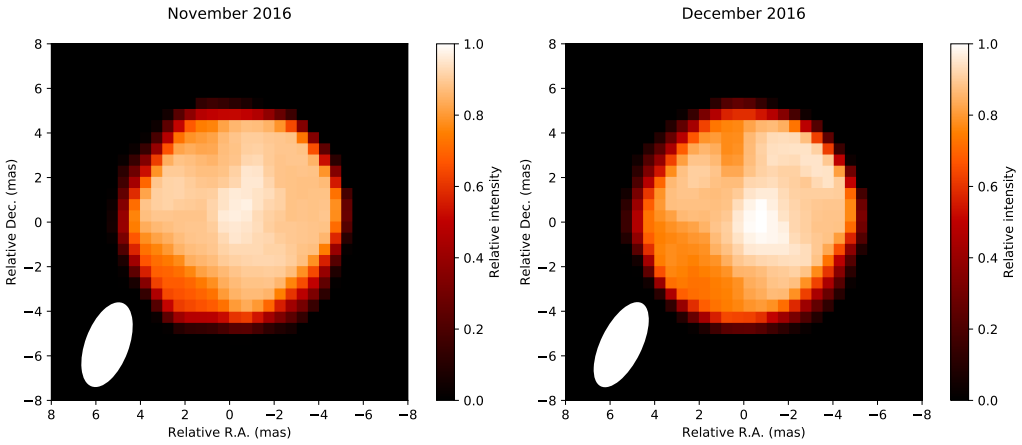

Fig. 2. Image reconstruction of the VLTI/PIONIER observations of CE Tau with the `SQUEEZE` algorithm. The white ellipse represents the synthesized beam (Montargès et al. 2018).

measured polarization is spatially integrated over the whole disc, its detection means a symmetry break in the layer emitting the polarized signal. This layer has to be close to the continuum forming region, below the formation of the atomic lines that cause the depolarization (see more details in Aurière et al. (2016)). The best interpretation is the presence of inhomogeneities in the photospheric region.

Fig. 3 top represents the probability of presence of a bright spot on the photosphere of Betelgeuse in January and November 2014. And Fig. 3 bottom represents a photospheric reconstruction of CE Tau based on the same technique (López-Ariste et al. subm.).

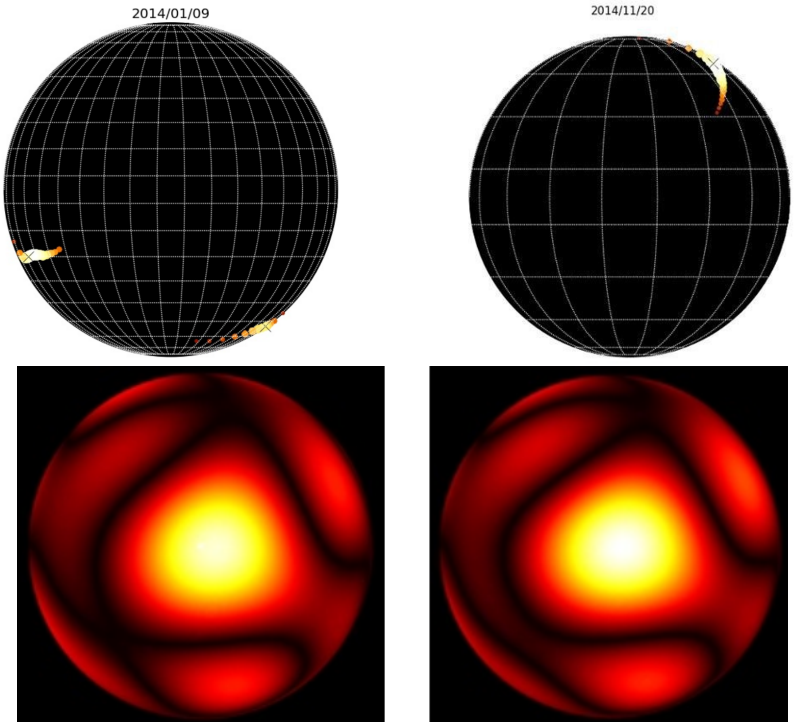

Fig. 3. Top: Probability of presence of a bright spot on the photosphere of Betelgeuse from visible spectropolarimetry in relative intensity (*left:* January 2014, and *right:* November 2014). **Bottom:** Reconstructed image of the photosphere of CE Tau using the same technique. The left image represents the November 2016 epoch, and the right image represents the December 2016 epoch .

While interferometry and spectropolarimetry imaging operates in different spectral domains (visible and near infrared), and while the analysis was conducted independently, it is noticeable that they reveal bright photospheric features on Betelgeuse and CE Tau at the same position, at the same time. Additionally, in the case of CE Tau, we note that the dark features are also matched

4 Conclusions

We presented evolution of photospheric features on the surface of RSG stars from NIR interferometric observations. These structures are interpreted as the top of convective cells using numerical simulations. Thanks to visible spectropolarimetry, the inhomogeneities on the surface of RSG can be tracked independently, thus confirming the interferometric observations.

The temporal series are crucial to understand the evolution and characteristics timescales of the convective features. Together with getting the photospheric velocity field of the photospheric features via interferometric high spectral resolution information (Ohnaka et al. 2017), and via tomography (Kravchenko 2018), these observations allow us to understand the dynamics of the photosphere of RSG.

Based on observations collected at the European Organisation for Astronomical Research in the Southern Hemisphere under ESO programs 288.D-5035(A), 090.D-0548(A), 092.D-0366(A), 092.D-0366(B), 094.D-0869 (A)298.D-5005(A) and 298.D-5005(B) and at the Télescope Bernard Lyot (TBL) at Observatoire du Pic du Midi, CNRS/INSU and Université de Toulouse, France. This project has received funding from the European Unions Horizon 2020 research and innovation program under the Marie Skłodowska-Curie Grant agreement No. 665501 with the research Foundation Flanders (FWO) ([PEGASUS]^2 Marie Curie fellowship 12U2717N awarded to M.M.). A.L. acknowledges financial support from "Programme National de Physique Stellaire" (PNPS) of CNRS/INSU, France. We used the SIMBAD and VIZIER databases at the CDS, Strasbourg (France)*, and NASA's Astrophysics Data System Bibliographic Services. This research has made use of the Jean-Marie Mariotti Center's `Aspro`† service, and of the `SearchCal` service‡ (co-developed by FIZEAU and LAOG/IPAG). This research made use of Matplotlib (Hunter 2007), Astropy§, a community-developed core Python package for Astronomy (Astropy Collaboration et al. 2013), and Uncertainties¶: a Python package for calculations with uncertainties.

References

Airapetian, V. S., Ofman, L., Robinson, R. D., Carpenter, K., & Davila, J. 2000, ApJ, 528, 965

Astropy Collaboration, Robitaille, T. P., Tollerud, E. J., et al. 2013, A&A, 558, A33

Aurière, M., Donati, J.-F., Konstantinova-Antova, R., et al. 2010, A&A, 516, L2

Aurière, M., López Ariste, A., Mathias, P., et al. 2016, A&A, 591, A119

Baron, F., Monnier, J. D., & Kloppenborg, B. 2010, in Proc. SPIE, Vol. 7734, Optical and Infrared Interferometry II, 77342I

Chiavassa, A., Freytag, B., Masseron, T., & Plez, B. 2011, A&A, 535, A22

Chiavassa, A., Haubois, X., Young, J. S., et al. 2010, A&A, 515, A12

Donati, J.-F., Semel, M., Carter, B. D., Rees, D. E., & Collier Cameron, A. 1997, MNRAS, 291, 658

Harper, G. M., Brown, A., Guinan, E. F., et al. 2017, AJ, 154, 11

Hunter, J. D. 2007, Computing In Science & Engineering, 9, 90

Josselin, E. & Plez, B. 2007, A&A, 469, 671

Kervella, P., Decin, L., Richards, A. M. S., et al. 2018, A&A, 609, A67

Kervella, P., Lagadec, E., Montargès, M., et al. 2016, A&A, 585, A28

Kravchenko, K. 2018, in Imaging of Stellar Surfaces, 20

Le Bouquin, J.-B., Berger, J.-P., Lazareff, B., et al. 2011, A&A, 535, A67

Mathias, P., Aurière, M., Ariste, A. L., et al. 2018, A&A, 615, A116

Meynet, G., Chomienne, V., Ekström, S., et al. 2015, A&A, 575, A60

Montargès, M., Kervella, P., Perrin, G., et al. 2016, A&A, 588, A130

Montargès, M., Kervella, P., Perrin, G., et al. 2014, A&A, 572, A17

*Available at `http://cdsweb.u-strasbg.fr/`
†Available at `http://www.jmmc.fr/aspro`
‡Available at `http://www.jmmc.fr/searchcal`
§Available at `http://www.astropy.org/`
¶Available at `http://pythonhosted.org/uncertainties/`

Montargès, M., Norris, R., Chiavassa, A., et al. 2018, A&A, 614, A12
O'Gorman, E., Kervella, P., Harper, G. M., et al. 2017, A&A, 602, L10
Ohnaka, K., Weigelt, G., & Hofmann, K.-H. 2017, Nature, 548, 310
Ohnaka, K., Weigelt, G., Millour, F., et al. 2011, A&A, 529, A163
Thiébaut, E. 2008, in Proc. SPIE, Vol. 7013, Optical and Infrared Interferometry, 70131I
Tremblay, P.-E., Ludwig, H.-G., Freytag, B., Steffen, M., & Caffau, E. 2013, A&A, 557, A7
van Leeuwen, F. 2007, A&A, 474, 653